A Study of Efficiency Dependence on Alloy Composition in an $Al_xGa_{1-x}As$ / $Al_xIn_{1-x}As$ Heterojunction Solar Cell: An Ultra Thin Film Approach

K. A. S. M. Ehteshamul Haque
Department of Electrical and Electronic Engineering, Islamic University of Technology
Board Bazar, Gazipur-1704, Bangladesh

Tahmid Nahian Bin Quddus
Department of Electrical and Electronic Engineering, Islamic University of Technology
Board Bazar, Gazipur-1704, Bangladesh

Mohammad Tanvirul Ferdaous
Department of Electrical and Electronic Engineering, Islamic University of Technology
Board Bazar, Gazipur-1704, Bangladesh

ABSTRACT
Variation in energy conversion efficiency in an $Al_xGa_{1-x}As$/ $Al_xIn_{1-x}As$ heterojunction solar cell has been studied by changing the alloy composition at different layers of the device. Simulations were done using Adept 1D software for different combinations of alloy composition of the layer materials, and light J-V characteristics curve was obtained for each combination. Energy conversion efficiency was calculated from light J-V characteristics curve (Under AM1.5G). The study was conducted by analysing the efficiency values resulting for different combinations. The best results were obtained for x= 0.9, 0.48 and 0.9 in the top, middle and bottom layers, respectively. For optimized values of layer thickness and doping concentration at different layers, this particular combination of alloy composition yielded an efficiency of 21.39% (under 1 sun). However, the device had two major drawbacks- lattice mismatch between adjacent layers, and high fabrication cost. These two issues have been taken care of later in the paper, and two low-cost, ultra-thin film solar cell designs were proposed.

Keywords
Ternary alloy, ultra-thin film solar cell, alloy composition, heterojunction, efficiency.

1. INTRODUCTION

1.1 Research Outlines
III-V ternary alloys are of particular interest as materials for heterojunction solar cells. The underlying reason here is the fact that their electrical properties such as bandgap, carrier mobility, dielectric constant [1] etc. can be greatly varied by changing their alloy compositions. This change also affects various optical properties like absorption coefficient [1], refractive index [2] etc. So, as constituents of solar cells, ternary alloys can offer great flexibility for optimization towards higher efficiency. In this paper, simulation results have been analyzed for varying alloy compositions of three ternary alloys- $Al_xGa_{1-x}As$, $Al_xIn_{1-x}As$ and $Ga_xIn_{1-x}As$, which constitute the top, middle and bottom layers, respectively, of a three-layer heterojunction solar cell. The top layer is n-doped, while the other two layers are p-doped. The whole structure rests on p-type Germanium (Ge) substrate. Figure 1 shows a schematic diagram of the device.

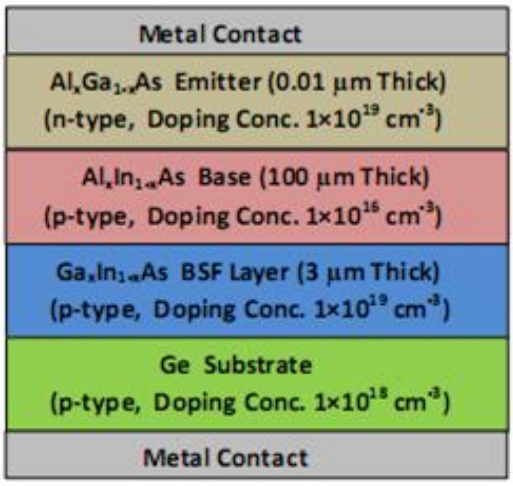

Fig 1: Schematic diagram of the $Al_xGa_{1-x}As$ / $Al_xIn_{1-x}As$ heterojunction solar cell with default parameters

The top layer material, $Al_xGa_{1-x}As$, can have a varying energy gap of 1.55-2.13 eV, as the Aluminium mole fraction x varies from 0.1 to 0.9. It becomes a direct bandgap material from an indirect one as x becomes lower, the transition point located at x= 0.45 [1]. Energy gap of the base layer material, $Al_xIn_{1-x}As$, varies from 0.5 to 2.05 eV, as x varies between 0.1 and 0.9 [3]. As x becomes higher, this material changes from a direct to indirect bandgap material, the transition point being located at $x \approx 0.63$ [3]. For $Ga_xIn_{1-x}As$, an energy gap variation between 0.43-1.28 eV is possible for variation of x (Gallium mole fraction) between 0.1-0.9 [4]. $Ga_xIn_{1-x}As$ is a direct material, for all values of x [1].

Now, the high fabrication cost of III-V solar cells is the major barrier to their use as terrestrial solar cells [5]. So, an ultra-thin film approach was finally taken to address this issue, where a trade-off was made between cell thickness and efficiency.

1.2 About the software
Adept [6] is a 1D simulation software that can simulate the output characteristics of heterostructured semiconductor devices. With this software, dark I-V characteristics, light I-V characteristics and spectral response of solar cells (or any other two-terminal device) can be computed.

2. METHODOLOGY

Before conducting simulations, some default values for thickness, doping concentration and alloy composition for each layer were fixed. Table 1 summarizes these default values.

Table 1. Default values of design parameters

Device Parameters	Top Layer	Middle Layer	Bottom Layer	Substrate
Layer Thickness (µm)	0.01	100	3	-
Doping Type	n	p	p	p
Doping Conc. (cm^3)	1×10^{19}	1×10^{16}	1×10^{19}	1×10^{18}
x value for the Alloy	0.7	0.48	0.67	-

Simulation was conducted with these default values, and the light J-V characteristics curve was obtained. From the curve, values of open-circuit voltage (V_{oc}) and short-circuit current density (J_{sc}) were noted. Fill factor was calculated [7] using equation (1).

$$FF = \frac{Vocn - \ln(Vocn + 0.72)}{Vocn + 1} \quad (1)$$

Where, $$Vocn = \left(\frac{q}{nkT}\right)Voc \quad (2)$$

Here,
V_{oc}= Open-circuit voltage (in Volt)
n= Ideality factor (taken as 1)
q= Charge of an electron
k= Boltzmann constant
T= Absolute Temperature (taken as 300 K)

To account for the incident sunlight, AM1.5G solar spectrum was considered in the simulation code. Using the values of V_{oc}, J_{sc}, FF and E (1000 W/ m^2), efficiency was calculated under 1 sun.

Now, simulations were conducted by varying the value of x for the top layer alloy ($Al_xGa_{1-x}As$) from 0.1 to 0.9, in steps of 0.1, and a plot of efficiency against x (Aluminium mole fraction) was obtained.

Similarly, efficiency vs mole fraction graph was obtained for $Al_xIn_{1-x}As$ and $Ga_xIn_{1-x}As$. Finally, after analysing these efficiency curves, three optimized designs were proposed.

Later on, the critical issue of lattice mismatch between adjacent layers was addressed with appropriate solutions. Finally, two low-cost, ultra-thin film solar cell designs were proposed.

3. RESULTS AND DISCUSSIONS

3.1 With Varying Alloy Composition in $Al_xGa_{1-x}As$ (Top Layer)

Aluminium mole fraction x, in $Al_xGa_{1-x}As$, was varied from 0.1 to 0.9, in steps of 0.1. Simulation was conducted in each case. The simulation outcomes are given in table 2, along with the energy gap values of $Al_xGa_{1-x}As$ for different alloy compositions. A plot of efficiency against corresponding values of x (Aluminium mole fraction) in $Al_xGa_{1-x}As$ is shown in figure 2.

Table 2. Simulation results for changing alloy composition of Aluminium Gallium Arsenide

x in $Al_xGa_{1-x}As$	Bandgap (eV)	J_{sc} (mA/cm^2)	V_{oc} (V)	FF
0.1	1.55	24.38	0.9531	0.8777
0.2	1.67	24.39	0.9523	0.8777
0.3	1.8	24.41	0.9532	0.8777
0.4	1.92	24.41	0.9534	0.8778
0.5	1.998	24.41	0.9534	0.8778
0.6	2.03	24.48	0.9535	0.8778
0.7	2.06	24.56	0.9535	0.8778
0.8	2.09	24.64	0.9534	0.8778
0.9	2.13	24.70	0.9535	0.8778

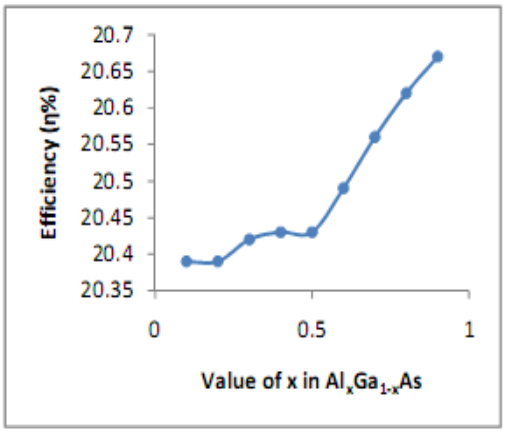

Fig 2: Graph of efficiency versus Aluminium mole fraction in $Al_xGa_{1-x}As$

The graph in figure 2 shows that higher efficiencies are obtained as the Aluminium mole fraction is increased in $Al_xGa_{1-x}As$. The top layer ($Al_xGa_{1-x}As$ layer) acts like a window layer [8] in the heterojunction solar cell. It is an established fact that the optical absorption in the base

(absorber) layer increases with higher bandgap of the window layer material [9, 10]. Higher optical absorption leads to higher output current and, as a result, higher efficiency. Now, it is seen from table 2 that the bandgap of $Al_xGa_{1-x}As$ increases with increasing Aluminium mole fraction (x) in the alloy. So, the efficiency is supposed to increase with increasing values of x, which is supported by the graph in figure 2. The irregularity in efficiency increment with increasing x is mainly due to the transition of $Al_xGa_{1-x}As$ from a direct to indirect material with increasing x [1].

3.2 With Varying Alloy Composition in $Al_xIn_{1-x}As$ (Middle Layer)

Aluminium mole fraction (x) in $Al_xIn_{1-x}As$ was varied from 0.1 to 0.6, in steps of 0.1. The simulation results are summarized in table 3. A plot of efficiency versus Aluminium mole fraction (x) in $Al_xIn_{1-x}As$ is given in figure 3. It is to be mentioned that simulations for x > 0.6 were not conducted, because $Al_{0.7}In_{0.3}As$ has an indirect bandgap of 1.85 eV [3], which is far from the optimum bandgap (1.4 eV) for the absorber of a solar cell [11].

Table 3. Simulation results for changing alloy composition of Aluminium Indium Arsenide

x in $Al_xIn_{1-x}As$	Bandgap (eV)	J_{sc} (mA/cm^2)	V_{oc} (V)	FF
0.1	0.5	55.92	0.075	0.4136
0.2	0.75	47.14	0.3087	0.7264
0.3	1.0	40.4	0.5408	0.814
0.4	1.23	31.4	0.7726	0.8568
0.5	1.48	23.29	0.9867	0.8809
0.6	1.75	16.71	1.0043	0.8825

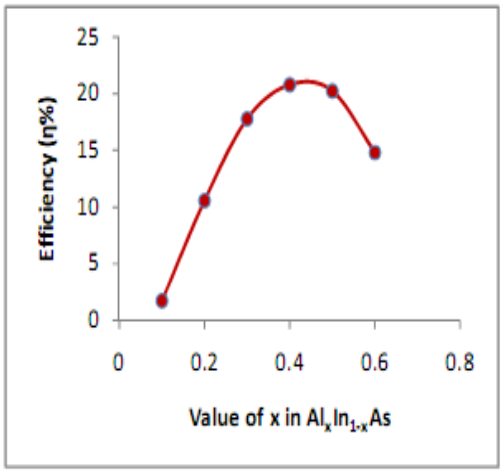

Fig 3: Graph of efficiency versus Aluminium mole fraction in $Al_xIn_{1-x}As$

The graph in figure 3 shows that maximum efficiency is obtained when Aluminium mole fraction in $Al_xIn_{1-x}As$ is between 0.4 and 0.5. Actually, this is the region where the bandgap of $Al_xIn_{1-x}As$ (1.23- 1.48 eV) is around the optimum value of 1.4 eV.

3.3 With Varying Alloy Composition of $Ga_xIn_{1-x}As$ (Bottom Layer)

Gallium mole fraction (x) in $Ga_xIn_{1-x}As$ was varied from 0.1 to 0.9, in steps of 0.1. The simulation outcomes are shown in table 4. Figure 4 plots the efficiency versus x in $Ga_xIn_{1-x}As$.

Table 4. Simulation results for changing alloy composition of Gallium Indium Arsenide

x in $Ga_xIn_{1-x}As$	Bandgap (eV)	J_{sc} (mA/cm^2)	V_{oc} (V)	FF
0.1	0.43	24.51	0.4347	0.783
0.2	0.50	24.51	0.5159	0.8076
0.3	0.59	24.51	0.6071	0.8289
0.4	0.68	24.52	0.7066	0.8469
0.5	0.78	24.53	0.8176	0.8627
0.6	0.89	24.55	0.9209	0.8745
0.7	1.01	24.56	0.9583	0.8782
0.8	1.14	24.59	0.9593	0.8783
0.9	1.28	25.2	0.9605	0.8785

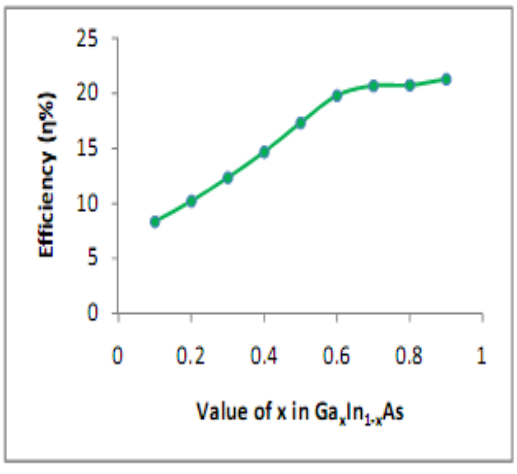

Fig 4: Graph of efficiency versus Gallium mole fraction in $Ga_xIn_{1-x}As$

It is evident from figure 4 that efficiency increases with increasing Gallium mole fraction in $Ga_xIn_{1-x}As$. Actually, the BSF layer plays little role in absorption, but the open-circuit

voltage increases slightly with increasing bandgap of the BSF layer [12, 13], and so the efficiency.

3.4 Optimization of Alloy Composition

3.4.1 First design

From the analysis of the efficiency curves, it was evident that x value in $Al_xIn_{1-x}As$ should be taken around 0.4, while x values for $Al_xGa_{1-x}As$ and $Ga_xIn_{1-x}As$ should be taken as high as possible. From this insight, a design was proposed for the heterojunction solar cell. For this particular design, x values in $Al_xGa_{1-x}As$, $Al_xIn_{1-x}As$ and $Ga_xIn_{1-x}As$ were taken as 0.9, 0.4 and 0.9, respectively. Figure 5 shows the light J-V characteristics graph obtained for this design.

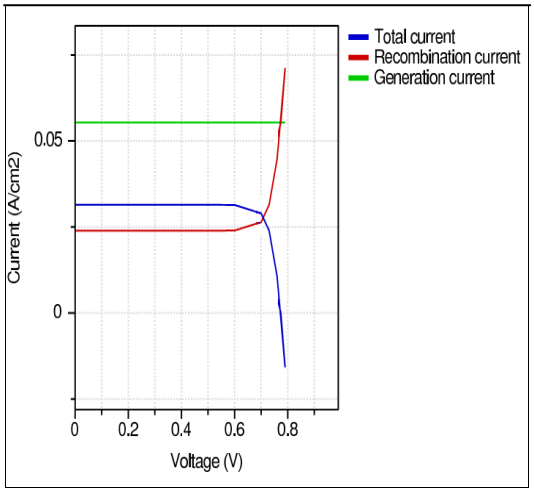

Fig 5: Light J-V characteristics of the first design

From figure 5, the open-circuit voltage (V_{oc}) is found to be 0.7739 V. The short-circuit current density (J_{sc}) is pretty high (31.47 mA/cm^2), and the calculated fill factor is 0.8569. The calculated efficiency is 20.87%. It is to be noted that a higher efficiency value was obtained during Gallium mole fraction variation in $Ga_xIn_{1-x}As$ (at x= 0.9). So, clearly, this design does not give the best level of optimization.

3.4.2 Second design

In this design, x in $Al_xIn_{1-x}As$ was taken as 0.5, while every other device parameter was kept the same as the first design. The light J-V characteristics graph obtained for this design is shown in figure 6.

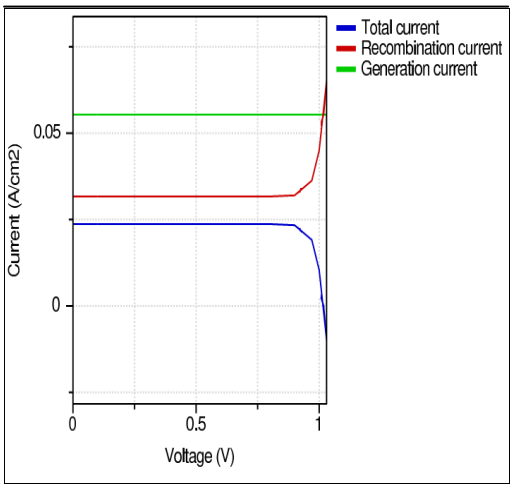

Fig 6: Light J-V characteristics of the second design

From figure 6, values of the open-circuit voltage (V_{oc}) and the short-circuit current density (J_{sc}) are found as 1.0179 V and 23.72 mA/cm^2, respectively. Clearly, the voltage has increased, but at the cost of a reduction in current. The calculated fill factor is 0.8837, and the resulting efficiency is 21.34%. So, the efficiency has increased as the Aluminium mole fraction in $Al_xIn_{1-x}As$ is taken to 0.5.

3.4.3 Third design

In this design, x in $Al_xIn_{1-x}As$ was taken as the default value (x= 0.48). Every other device parameter was kept the same as the first design. Figure 7 shows the light J-V characteristics graph obtained for this design.

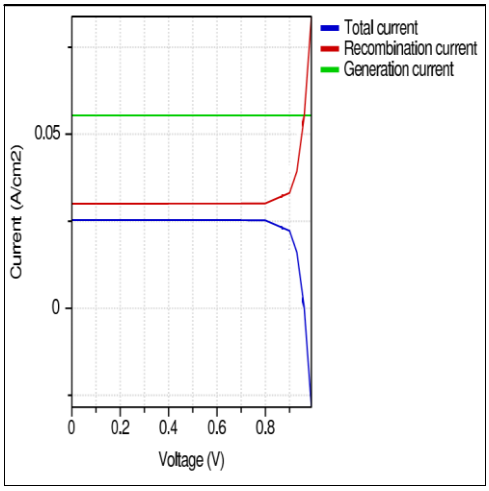

Fig 7: Light J-V characteristics of the third design

For the third design, the obtained open-circuit voltage is 0.9607 V, while the short-circuit current density is 25.34 mA/cm^2 (from figure 7). The calculated fill factor is 0.8785. Finally, the calculated efficiency is 21.39%. This is highest efficiency achieved from the three proposed designs.

3.5 Problems in the Proposed Designs

3.5.1 Lattice mismatch

The major problem in the proposed designs is the high lattice mismatch between the layers. Germanium has a lattice constant of 5.65 Å [14]. Now, the growth of $Ga_{0.9}In_{0.1}As$ on Ge demands perfect lattice-matching between these two materials. But the lattice constant of $Ga_{0.9}In_{0.1}As$ is 5.6938 Å [1], which results in a lattice mismatch of 0.77% with Ge. Though the mismatch is small, it restricts the growth of $Ga_{0.9}In_{0.1}As$ on Ge to a critical layer thickness of 12 nm [15].

$Al_{0.48}In_{0.52}As$ has a lattice constant of 5.8686 Å (lattice-matched with InP [10]). So, the lattice mismatch between $Ga_{0.9}In_{0.1}As$ and $Al_{0.48}In_{0.52}As$ is 2.98%, which is pretty high, and gives a critical layer thickness of 2 nm only [15].

$Al_{0.9}Ga_{0.1}As$ has a lattice constant of 5.66032 Å [1], and the lattice mismatch between $Al_{0.9}Ga_{0.1}As$ and $Al_{0.48}In_{0.52}As$ is 3.55%. This gives a critical layer thickness around 2 nm for epitaxial growth [15].

3.5.2 High fabrication cost

The designs proposed in section 3.4 yield nearly the maximum possible efficiency for this particular heterojunction solar cell, but the issue of material and fabrication cost was not considered while proposing the designs. The fabrication cost of ternary III-V compounds is high [16], and bulk III-V

solar cell is not a cost-effective option. So, a trade-off between efficiency and material cost is necessary in the designs being proposed.

3.6 Practical, Cost-effective Designs

3.6.1 Solving the lattice mismatch issue

One way to solve the lattice mismatch problem between two adjacent layers is to apply a buffer layer in between, which will have an intermediate lattice constant. The ideal lattice constant of a buffer layer that can be applied between $Al_{0.48}In_{0.52}As$ and $Ga_{0.9}In_{0.1}As$ is around 5.78 Å, which still generates 1.5% lattice mismatch with the $Al_{0.48}In_{0.52}As$ layer, and gives a critical thickness of around 7 nm only [15]. But the $Al_{0.48}In_{0.52}As$ absorber must be sufficiently thick, and the defect-free growth of a thick $Al_{0.48}In_{0.52}As$ layer on a material requires perfect lattice-matching between them. So, using a buffer layer between $Al_{0.48}In_{0.52}As$ and $Ga_{0.9}In_{0.1}As$ cannot be a solution.

Before solving the lattice mismatch issue of $Al_{0.9}Ga_{0.1}As$ and $Al_{0.48}In_{0.52}As$, it should be mentioned that an ultra-thin window layer improves the performance of solar cell [17]. So, a buffer layer between $Al_{0.9}Ga_{0.1}As$ and $Al_{0.48}In_{0.52}As$ is not actually needed, rather an ultra-thin layer of $Al_{0.9}Ga_{0.1}As$ can be considered, which has a thickness equal to the critical layer thickness in this case (2 nm).

Now, the lattice mismatch issue between $Al_{0.48}In_{0.52}As$ and $Ga_{0.9}In_{0.1}As$ is being addressed. It is to be noted that $Ga_{0.47}In_{0.53}As$ is perfectly lattice matched to $Al_{0.48}In_{0.52}As$ [2]. Now, section 3.3 suggests that reducing the Gallium mole fraction in $Ga_xIn_{1-x}As$ degrades the efficiency of the solar cell; still, this approach has to be followed in order to ensure perfect lattice matching between the absorber and the BSF layer, so that the absorber can be grown in any desired thickness. So, $Ga_{0.47}In_{0.53}As$ will be used as the BSF layer material in the practical designs proposed in sections 3.6.2 and 3.6.3. $Ga_{0.47}In_{0.53}As$ has a direct bandgap of 0.7734 eV.

A new problem arises that the lattice mismatch between $Ga_{0.47}In_{0.53}As$ and Ge is higher (3.7%) than it was for $Ga_{0.9}In_{0.1}As$. This gives a critical layer thickness for the growth of $Ga_{0.47}In_{0.53}As$ on Ge of slightly less than 2 nm [15].

3.6.2 Cost-effective solar cell- a thin film approach

As it was mentioned in section 3.5.2, a trade-off is needed to be made between cell efficiency and material cost. Now, using 2 nm thick emitter and BSF layers have already been decided, for eliminating the effect of lattice mismatch. So, the highest efficiency design discussed in section 3.4.3 is brought back with three modifications- using $Ga_{0.47}In_{0.53}As$, instead of $Ga_{0.9}In_{0.1}As$, for the BSF layer, changing the top layer thickness to 2 nm, and changing the BSF layer thickness to 2 nm. Figure 8 shows the light J-V characteristics curve for this design.

The short-circiut current density for this design is 28.47 mA/ cm^2, open-circuit voltage is 0.7063 V, and the fill factor (FF), calculated using equation (1) is 0.8469. The calculated efficiency is 17.03%. It is seen that the efficiency is decreased significantly, compared to the 21.39% efficiency in section 3.4.3, due to the reasons already discussed.

Now, a number of simulations have been conducted with varying base layer thickness values, in order to provide a good number of options for the efficiency and cost trade-off. Table 5 lists the simulation outcomes. A graph of efficiency versus middle layer thickness of the modified design is shown in figure 9.

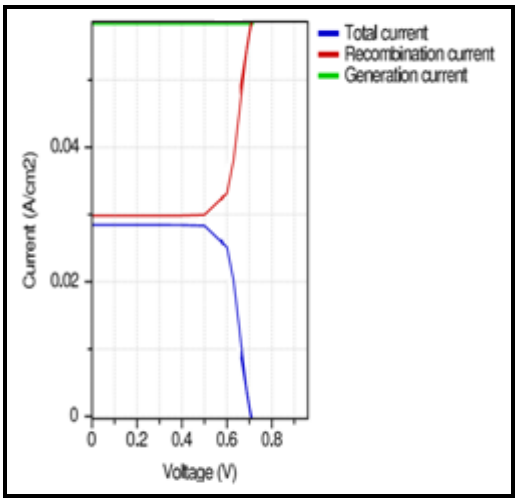

Fig 8: Light J-V characteristics curve for the modified design

The results shown in table 5 give few good design options that are cost-effective and moderately efficient. It is to be noted that thickness of the emitter and base (2 nm each) are negligible, when the base thickness is in the range of microns. So, the base thickness can be considered as the thickness of the cell (excluding the substrate thickness).

Table 5. Simulation results for varying base thickness of the modified design

Base Thickness (µm)	J_{sc} (mA/cm^2)	V_{oc} (V)	FF
100	28.47	0.7063	0.8469
20	28.33	0.6419	0.8357
10	28.13	0.6208	0.8317
5	27.66	0.6004	0.8275
2	25.95	0.5706	0.821

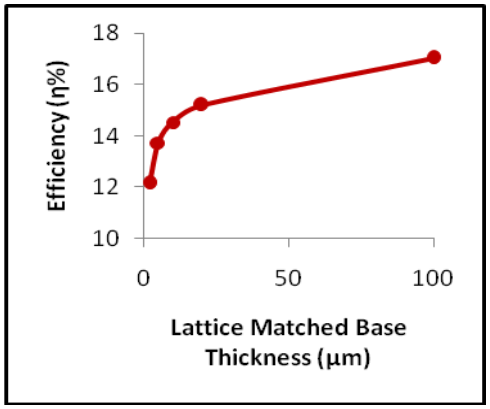

Fig 9: Efficiency vs absorber thickness of the modified design

It is seen from table 5 that a 10 µm thick cell yields an efficiency of 14.52%. The 5 µm cell can be an option as a thin film solar cell, which yields an efficiency of 13.74%. For a better thin film approach, the 2 µm cell can be considered, which gives an efficiency of 12.16%. The light J-V characteristics curve for the 2 µm cell thickness design is given in figure 10.

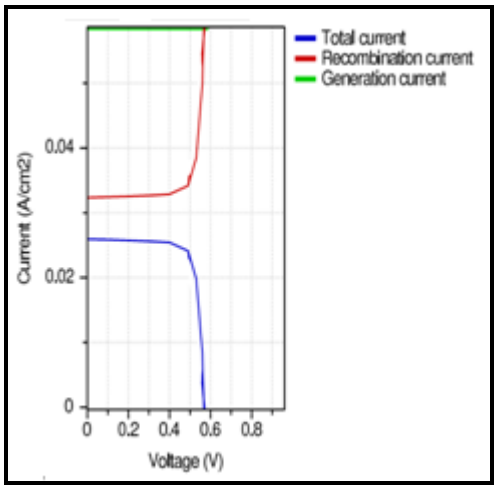

Fig 10: Light J-V characteristics curve for 2 µm cell thickness (excluding substrate thickness)

3.6.3 A better approach

From the proposed cost-effective designs in section 3.6.2, it is noticed that the efficiency is decreased, compared to the design of section 3.4.3. This is mainly due to the low bandgap of $Ga_{0.47}In_{0.53}As$ (0.7734 eV), compared to that of $Ga_{0.9}In_{0.1}As$ (1.28 eV). But the necessity of perfect lattice matching between the two materials ($Al_{0.48}In_{0.52}As$ and $Ga_xIn_{1-x}As$) cannot be compromised. So, x value in $Ga_xIn_{1-x}As$ must be kept at 0.47. Now, in order to improve the output characteristics, the use of an InP substrate is suggested, instead of Ge. InP is perfectly lattice-matched to $Al_{0.48}In_{0.52}As$ and $Ga_{0.47}In_{0.53}As$. Though InP is costlier than Ge [18], using InP substrate for this solar cell is advantageous for two reasons- InP has a much higher bandgap (1.344 eV) than Ge, which improves the open-circuit voltage slightly; and the BSF layer can now be grown at any desired thickness. An ultra-thin BSF layer slightly degrades the efficiency of the cell.

Considering the issue of cost-effectiveness, the very final design of the solar cell is suggested, where the $Al_{0.48}In_{0.52}As$ absorber is 2 µm thick, and the $Ga_{0.47}In_{0.53}As$ BSF layer will have a thickness of 1 µm. The solar cell will be grown on InP substrate, instead of Ge. Every other design parameter is kept the same as the 2 µm solar cell, discussed in section 3.6.2. Simulation was conducted for this cell, and the light J-V characteristics curve is given in figure 11.

It is noted that this solar cell has a total thickness of 3 µm (excluding the substrate thickness). The short-circuit current density (J_{sc}) was obtained as 26.03 mA/cm^2. The open-circuit voltage was 0.637 V, and the fill factor (FF) was 0.8348. The efficiency was calculated as 13.84%. Clearly, with this design, the open-circuit voltage is considerably improved, and so the efficiency, compared to the 2 µm solar cell.

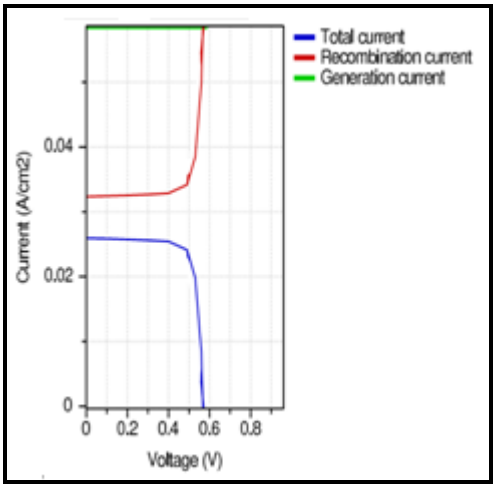

Fig 11: Light J-V characteristics curve for the 3 µm cell on InP substrate

4. CONCLUSIONS

In this work, the dependence of energy conversion efficiency on alloy composition has been investigated in details for the $Al_xGa_{1-x}As$ / $Al_xIn_{1-x}As$ heterojunction solar cell. The results found in this paper can provide a better insight into the way of alloy composition optimization in heterojunction and multijunction solar cells fabricated from ternary and quaternary alloys for achieving the highest possible efficiency. The paper also discusses the critical fabrication issues of this particular solar cell, and proposes practical and cost-effective designs. The final significant contribution made in this paper is the design of an ultra-thin film solar cell with moderate efficiency. The advantage of InP over Ge as a substrate for this particular solar cell has also been demonstrated.

5. ACKNOWLEDGMENTS

The authors would like to thank Shah Mohammad Bahauddin, Dept. of Applied Physics, Electronics and Communication Engineering (APECE), University of Dhaka, for offering a helpful introduction with Adept software.

6. REFERENCES

[1] Ioffe Physical Technical Institute. 2005. NSM Archive - Physical Properties of Semiconductors. http://www.ioffe.ru/SVA/ NSM/Semicond/

[2] ECEn IMMERSE Web Team, Brigham Young University. 2009. Energy Gap in III-V Ternary Semiconductors. http://www. cleanroom.byu.edu /EW_ternary.phtml

[3] N. Bouarissa and M. Boucenna,. 2009. Band parameters for AlAs, InAs and their ternary mixed crystals. Physica Scripta, vol. 79, pp. 0157011-0157017.

[4] K. H. Goetz, D. Bimberg, H. Jurgensen, J. Selders, A.V.Solomonov, G.F.Glinskii and M. Razeghi. 1983. Optical and crystallographic properties and impurity incorporation of $Ga_xIn_{1-x}As$ ($0.44<x<0.49$) grown by liquid phase epitaxy, vapor phase epitaxy, and metal organic chemical vapor deposition. Journal of Applied Physics, vol. 54, pp. 4543- 4552.

[5] M. Bosi and C. Pelosi. 2007. The Potential of III-V Semiconductors as Terrestrial Photovoltaic Devices. Progress in Photovoltaics: Research and Applications, vol. 15, pp. 51-68.

[6] J. L. Gray and Michael McLennan. 2008. Adept. http://nanohub.org/resources/adept/

[7] M. A. Green. 1981. Solar cell fill factors: General graph and empirical expressions. Solid-State Electronics, vol. 24, pp. 788-789.

[8] Harish Palaniappan. 2012. Solar Cells. http://solar_cells.tripod.com/notes_sel_1.html

[9] U. S. Department of Energy. 2011. Energy Basics. http://www.eere.energy.gov/basics/renewable_energy/pv_cell_structures.html

[10] M. S. Leite, R. L. Woo, W. D. Hong, D. C. Law and H. A. Atwater. 2011. Wide-band-gap InAlAs solar cell for an alternative multijunction approach. Applied Physics Letters, vol. 98, pp. 0935021-0935023.

[11] T. Tiedje, E. Yablonovitch, G. D. Cody and B. G. Brooks. 1984. Limiting efficiency of silicon solar cells. IEEE Transactions on Electron Devices, vol. 31, pp. 711-716.

[12] P. K. Nayak, G. G. Belmonte, A. Kahn, J. Bisquert and D. Cahen. 2012. Photovoltaic efficiency limits and material disorder. Energy and Environmental Science, vol. 5, pp. 6022-6039.

[13] K. Van Nieuwenhuysen, F. Duerinckx, I. Kuzma, D. van Gestel, G. Beaucarne and J. Poortmans. 2006. Progress in epitaxial deposition on low-cost substrates for thin-film crystalline silicon solar cells at IMEC. Journal of Crystal Growth, vol. 287, pp. 438-441.

[14] B. G. Streetman and S. K. Banerjee. 2006. Solid State Electronic Devices (6th Ed.). Prentice-Hall Inc., New Jersey, USA.

[15] J.W. Matthews and A.E. Blakeslee. 1974. Defects in epitaxial multilayers: I. Misfit dislocations. Journal of Crystal Growth, vol. 27, pp. 118-125.

[16] H. J. Scheel and P. Capper. Crystal Growth Technology: From Fundamentals and Simulation to Large-scale Production (1st Ed.). 2008. Wiley-VCH Verlag GmbH & Co. KGaA, Weinheim, Germany.

[17] M. S. Hossain, N. Amin, M. A. Matin, M. M. Aliyu, T. Razykov and K. Sopian. 2011. A numerical study on the prospects of high efficiency ultra thin $Zn_xCd_{1-x}S$/ CdTe solar cell. Chalcogenide Letters, vol. 8, pp. 263-272.

[18] A.W. Bett, F. Dimroth, G. Stollwerck and O.V. Sulima. 1999. III-V compounds for solar cell applications. Applied Physics A, vol. 69, pp. 119-129.